Titanium Implants after Alkali Heating Treatment with a $[Zn(OH)_4]^{2-}$ Complex: Analysis of Interfacial Bond Strength Using Push-Out Tests

Kelly Alvarez, PhD;* Masayuki Fukuda, DDS, PhD;† Osamu Yamamoto, PhD‡

ABSTRACT

Background: Clinical demands for stronger and faster bone bonding to implants have motivated the development of chemically and topographically modified surfaces capable of chemical bonding. This study presents a new one-step alkali heat treatment performed with a solution containing $[Zn(OH)_4]^{2-}$ complex as an alternative to the conventional NaOH solution.

Purpose: The objective of this work is to assess the effect of a Zn-modified surface chemistry on bone-implant shear strength using a rabbit model.

Materials and Methods: The study was conducted on mechanical-grinded and smooth surfaces of Ti cylindrical implants. The topographical structure, chemical surface composition, and structural properties of the chemically modified titanium surface were studied by scanning electron microscopy, x-ray photoelectron spectroscopy, and x-ray diffractometry. Implant-bone shear strength was evaluated by push-out tests undertaken at 4, 12, and 24 weeks after insertion in rabbit femora.

Results: Implants with smooth and rough surfaces chemically-modified with a solution containing $[Zn(OH)_4]^{2-}$ complex demonstrated significantly stronger bone fixation than nonmodified implants at all healing times ($p < 0.05$).

Conclusions: The obtained results suggest that biochemical bonding at the bone-implant interface, stimulated by the Zn^{2+} ion release in combination with mechanical interlocking definitively improved the implant fixation.

KEY WORDS: biomechanical test, surface modification, titanium, Zn^{2+} ion-incorporated Ti implant, $[Zn(OH)_4]^{2-}$ complex alkali heating

INTRODUCTION

Many surface modifications have been developed to enhance the bone bonding ability of titanium-based implants. Among them, alkali heating and subsequent high-temperature heat treatment is one of the most successful and easy treatments to generate a modified surface that induces the formation of bone-like apatite. Yang and colleagues in 1997 and Fujibayashi and colleagues in 2001 reported that sodium hydroxide heat-treated sodium-incorporated implants exhibited significantly higher failure loads in rabbit tibiae.[1,2] When the alkali heat-treated Ti was implanted into the tibiae of rabbits, it formed a Ca and P-rich layer at the Ti-bone interface. At the scanning electron microscope level this layer directly bonded to the host bone at an early post-operative period. In contrast, the untreated Ti during the early postimplantation period just exhibited a fibrous layer between the Ti implant and bone, and direct contact with the bone was observed only after 16 weeks.[1] Therefore, mechanical evaluation of the bone-bonding strength resulted in being significantly higher in the alkali heat-treated Ti implants.

---

*Doctorate fellow, Center for Geo-Environmental Science, Faculty of Engineering and Resource Science, Akita University, Akita, Japan; †professor, Division of Dentistry and Oral Surgery, Akita University Hospital, Akita, Japan; ‡professor, Center for Geo-Environmental Science, Faculty of Engineering and Resource Science, Akita University, Akita, Japan

Reprint requests: Prof. Osamu Yamamoto, Center for Geo-Environmental Science, Faculty of Engineering and Resource Science, Akita University, 1-1 Tegata Gakuen-machi, Akita 010-8502, Japan; e-mail: yamamoto@cges.akita-u.ac.jp

DOI 10.1111/j.1708-8208.2010.00278.x

Recent discoveries have revealed that bone regeneration in close proximity to implant surfaces requires bone-repairing materials capable of providing biochemical signals to promote bone formation at the cellular level. If appropriate bone-inducing substances or essential elements are intentionally present at the biomaterial surface, they may provide signals to a selected type of cells to promote their adhesion or positively affect their function. The incorporation of trace essential elements into biomaterials has proven to be an effective way to stimulate bone formation.[3–5] Studies in vitro and in vivo have demonstrated that zinc (Zn) is able to stimulate bone formation and to inhibit bone resorption.[6–8] However, Zn must be released slowly from the implant surface because Zn at elevated levels induces adverse reactions.

The cellular mechanism of Zn has been partially elucidated. Zn ion inhibited the formation of osteoclastic cells from bone marrow cells,[9,10] and could also reduce pit formation by isolated neonatal rat osteoclasts in a biphasic matter without having effect on the osteoclasts number.[11] Meanwhile, Zn ion has been demonstrated to have a stimulative effect on bone formation and mineralization in osteoblastic cell cultures because of the promotion of bone cellular protein synthesis.[12,13]

On the other hand, surface topography also influences the rate at which bone is formed next to the implant surface. It has been reported that roughened dental implants show a stronger bone response than turned dental implants.[14] In vivo studies have demonstrated also that bone-implant contact was different depending on weather the surface was electropolished (smooth) or machined (rough), even though the Ti surfaces were of similar oxide thickness.[15]

The present study was conducted to determine whether a zinc ion (Zn^{2+})-containing alkali heat treatment to chemically modify the surface of Ti implants would accelerate the rate of new tissue formation improving also the interfacial implant-bone bond strength. We combined the Zn-modification with a mechanical grinding treatment (MGT), in order to induce a synergetic biological effect. Our hypotheses were: (1) an alkali heat treatment containing $[Zn(OH)_4]^{2-}$ complex would remarkably enhance the bone-implant fixation and (2) a dual chemical and topographical modification would lead to a stronger bone-implant fixation than a chemical modification alone. These questions were addressed by employing push-out tests undertaken at 4, 12, and 24 weeks after the implant insertion in rabbit femora to evaluate the implant-bone shear strength of the different chemically and topographically modified Ti surfaces. By means of several surface analysis techniques, a detailed surface characterization of the different modifications applied was drawn in order to relate the surface characteristics with the achieved implant fixation of the fabricated chemically and topographically modified implants. Measurements of the implant-bone shear strength demonstrated that the newly proposed one-step alkali heat treatment containing $[Zn(OH)_4]^{2-}$ complex increased the biochemical bonding at the bone-implant interface, probably stimulated by the Zn^{2+} ion release in combination with the mechanical interlocking achieved by the topographical modification. Therefore, this novel surface modification seems to be a simple and effective method not only to induce apatite formation on a Ti surface, but also to stimulate bone formation and mineralization after osteoplasty.

MATERIALS AND METHODS

Sample Preparation and Surface Modification

For the alkali heat treatment cylindrical samples (Ø 2 mm, 5 mm length) of as received commercially pure-titanium metal (cp-Ti > 99.9%) (Nilaco Co., Tokyo, Japan) were used. The samples were ultrasonically cleaned with ethanol and distilled water and dried at 70°C for 10 min. The alkali solution containing the $[Zn(OH)_4]^{2-}$ complex was prepared by dissolving under constant stirring 14.85 g of reagent-grade zinc nitrate hexahydrate ($Zn(NO_3)_2{\cdot}6H_2O$) (99%, Nacalai Tesque, Kyoto, Japan) and 24.00 g of reagent-grade sodium hydroxide (NaOH) (96%, Nacalai Tesque, Kyoto, Japan) in distilled water to form a 100 mL solution [$Zn^{2+} = 0.5$ M, $OH^- = 6.0$ M]. At the beginning of the process, a $Zn(OH)_2$ precipitate is obtained and the solution becomes milky and turbid. However, when an additional of 4.0 g of NaOH is added, the $Zn(OH)_2$ precipitate dissolved to yield a homogeneous transparent solution containing $[Zn(OH)_4]^{2-}$ complex through the reaction: $Zn(OH)_2 + 2OH^- \rightarrow [Zn(OH)_4]^{2-}$.

The samples were soaked with stirring in 300 mL of this solution in Teflon® beakers (ASONE Co., Tokyo, Japan) for 24 hours at 60°C. After the soaking period the $[Zn(OH)_4]^{2-}$ complex solution remains transparent without any precipitation. This alkali treatment is performed to induce the apatite forming ability and at the same time generate a Zn^{2+} ion releasing titanium surface. At the end of the soaking period, the implants were washed thoroughly for 1 minute with running distilled water and dried inside an electric furnace at 70°C for 30 minutes. Pure Ti rods without any surface treatment were used as control. The samples were separated into four groups, each one with five implants for each healing time, as follows:

- group I, cp-Ti smooth surface (control group)
- group II, cp-Ti mechanically grinded surface
- group III, Zn-modified Ti, smooth surface
- group IV, Zn-modified Ti, mechanically grinded surface

The MGT of the titanium surface was carried out in order to generate a micrometer order surface roughness and consequently improve the osseointegration, fixation and stability of the implant. The cylindrical implants were abraded with an electric micro grinding machine (Urawa Manufacturing Co. Ltd, Saitama, Japan). The MGT was conducted at room temperature without coolant, turning the titanium workpiece around its own axis of rotation at a rotation speed of 16 rpm and abrading it by means of a resin-bonded silica sand wheel rotating at 3.35 m/s (8000 rpm). Following the MGT, the implants were washed with pure acetone and distilled water in an ultrasonic cleaner.

Implant Surface Evaluation and Zn Ion Release Test

Surface morphologies of the specimens after alkali treatment in the solution containing the $[Zn(OH)_4]^{2-}$ complex were observed by field emission scanning electron microscopy (FESEM; HITACHI S-4500) at an operating voltage of 20 kV. Elemental analysis of the surface was carried out by FESEM equipped with an energy dispersive x-ray analyzer (EDX; (HORIBA, EMAX-7000, Japan). The effect of the surface treatment was analyzed by thin film x-ray diffractometry (TF-XRD) (RINT 2000, Rigaku Co., Tokyo, Japan). The x-ray incident angle to the specimens was fixed at 2°. The compositions of the outermost film were analyzed by x-ray photoelectron spectroscopy (XPS; ESCA 5600, Perkin-Elmer Co., USA). Monochromatic Al K_α radiation (1486.6 eV) was used as the x-ray source. Acquisition conditions were 13 kV, 400 W source power, and 94 eV pass energy. All spectra were collected at a photoelectron takeoff angle of 45°. High-resolution scans were run for Ti, Zn, and O using an x-ray beam with about 15 nm diameter. The XPS depth profile measurement was performed after Ar^+ ion etching at etching rate of 2 nm/min. Ar^+ ion etching was performed with a rapid etching ion gun mounted inside the UHV chamber of the XPS machine operated at 3 KeV. Ar^+ ion bombardment angle was 90° and XPS spectra were measured after Ar^+ ion bombardment each time. As reference materials, steam sterilized Ti samples were subjected to the same XPS and TF-XRD analyses.

The surface roughness was examined by profilometry using a surface texture and contour-measuring instrument (SURFCOM 3000A, Tokyo Seimitsu Co. Ltd, Japan). The recorded surface profiles were digitalized and the relevant surface parameters: centerline average (R_a) and peak to valley height (R_z) within a sampling length (S_L) of 2 mm were determined using a special computer program. The surface roughness measurements were performed at three different points on each type of sample to obtain an average value and a standard deviation.

In order to quantify the dissolution behavior of the Zn ions, 10 titanium specimens immersed in the alkali solution containing the $[Zn(OH)_4]^{2-}$ complex solution were soaked in 100 mL of physiological saline solution (0.9% NaCl, pH 7.4) and placed in a mechanical shaker bath at 37°C for predetermined periods of time (3, 6, 24, 48, 72, and 168 hours). At the end of each soaking period, a 10 mL aliquot was removed and the Zn^{2+} ion concentration released from 10 samples was measured without dilution using an Inductively Coupled Plasma Atomic Emission Spectrometry instrument (ICP-AES, SPS 7700, Seiko Instruments Inc., Japan), using the emission line at 202.548 nm. The zinc detection limit was 0.012 ppm.

Surgical Placement of the Implants

The Animal Research Committee of Akita University, Akita, Japan, approved the protocols for animal experimentation described in this study; all subsequent animal experiments strictly adhered to the "Guidelines for Animal Experimentation" of the University. Nine adult male, skeletally mature Japanese white rabbits, weighing 3.5 to 4.0 kg were used. The animals were anesthetized with sevofrane (Maruishi Pharmaceutical Co., Osaka, Japan) 14 mL/kg.

Each rabbit was anesthetized with an intramuscular injection of 4 mL of a 3:1 mixture of Ketamine hydrochloride (30 mg/kg, Ketalar 200 mg; Sankyo Co., Ltd, Tokyo, Japan) and Xylazine hydrochloride (10 mg/kg, Sedeluck, Zenoaq, Fukushima, Japan).

One thousand eight hundred micro liters of local anesthetic, 2% lidocaine hydrochloride containing 1:80,000 epinephrine (Xylocaine Poly Amp 2% (Fujisawa Pharmaceutical Co., Ltd, Osaka, Japan) was administered around the femur at each implant site.

After 4, 12, and 24 weeks the rabbits were generally anesthetized as described above, and an overdose of pentobarbitalum natricum (50 mg/kg intravenously, Nembutal, Dainippon Pharmaceutic Co., Ltd, Osaka, Japan) was delivered intravenously to sacrifice the animals. For each time point, five cylindrical implants, which surface was previously modified by immersion into the alkali solution containing the $[Zn(OH)_4]^{2-}$ complex, were used in each rabbit along with five unmodified control implants. Each implant had a length of 5 mm and diameter of 2 mm and one of two surfaces, smooth or abraded were used in this experiment. Before the surgery the implants were sterilized via dry-heat sterilization carried out at 180°C for 2 hours in a dry-heat thermostated oven. Under sterile surgical conditions, an incision of approximately 6 cm in length was made to expose the mid-diaphyseal region of the femur. By dissecting femoral muscles and periosteum, a unicortical defect (Ø 2 mm), perpendicular to the longitudinal axis of the diaphysis was created. A low-speed dental drill, which had a drill bit the same size as the inserted implants, was used to make a hole through the bone into the bone marrow. The hole was drilled under generous physiological saline solution irrigation to avoid overheating of the bone. The implants were press-fitted into the prepared holes to the full-length unicortically, after cooling the cavities with physiological saline solution to remove bone debris (Figure 1). Each rabbit received five implants from one of the test groups in a both the left and right femurs condyle close to the knee joint. The muscular tissue was sutured with absorbable thread and the skin with mononylon 4–0 surgical thread. The animals were allowed to recover from anesthesia in the operation room and were then housed individually in cages that allowed some movement with free access to food and water. The animal's legs were load bearing after the surgical placement of the implants.

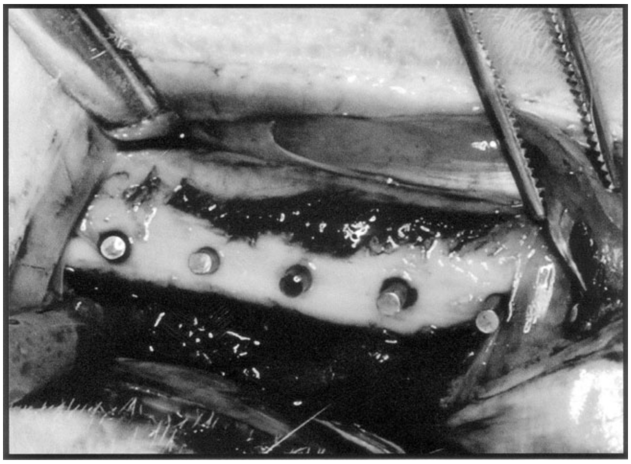

Figure 1 Intraoperative photograph showing the transcortical cylindrical implants inserted in the femoral cortex of rabbit. The long axis of the implants was perpendicular to the long axis of the femur. 109 × 80 mm (300 × 300 DPI).

Biomechanical Testing and SEM Observation

To determine the bone-implant interface attachment strength mechanical push-out testing was done. A detailed description of the method and a schematic diagram of the arrangement used for the mechanical tests can be found in Bobyn and colleagues[16] and Nishiguchi and colleagues.[17] At the end of each implantation period, freshly excised specimens were cleaned of soft tissue and were transported on ice to the laboratory. Bone segments of about 2 cm containing one implant were cut from the femoral diaphysis perpendicular to the long axis of the femur using a water-cooled diamond saw. Afterwards, the five bone-implant sites containing one implant each were bisected radially through the medullary cavity of the femur, separating the half of the cortex that was not penetrated by the implant. After the sectioning, the samples were kept in 0.15 M saline solution at 4°C until the next day. All tests were carried out within 24 hours after sacrificing the animals. During this time period, the bone specimens kept moist with cold saline solution and before the mechanical testing were equilibrated at room temperature. The biomechanical tests were carried out by placing the femoral segments on a support metallic jig using a computer-controlled universal testing machine (Autograph AGS-J, Shimadzu Corp., Kyoto, Japan) at a crosshead speed of 0.5 mm/min until the peak force resulting in the detachment of the bone (F_{max}) was obtained. The supporting jig was mounted on the lower jaw of the testing machine and a metallic load applicator of 3 mm in diameter was fixed vertically to the upper jaw ensuring that for each testing the applied load was parallel to the implant's long axis. All force data was converted to nominal

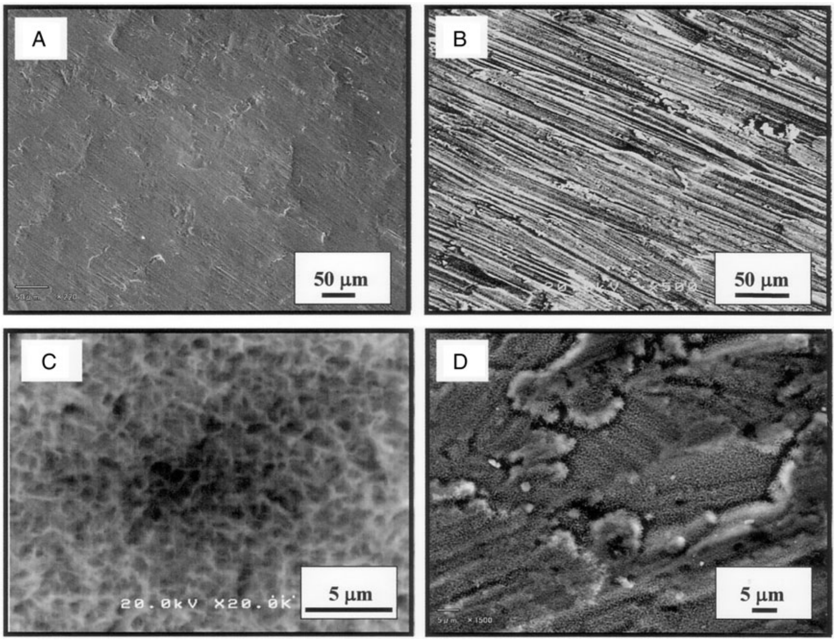

Figure 2 SEM micrographs showing the surface morphologies of the tested Ti and Zn-modified Ti samples: group I (A), group II (B), group III (C), group IV (D). 166 × 130 mm (200 × 200 DPI).

stress values using the measured cross-sectional area of each implant. The shear strength at the interface (MPa) is defined as:

$$\sigma = F_{\max}/(\pi DT) \qquad (1)$$

where d is the diameter of the cylinder-type implant (mm) and t is the mean thickness of the compact bone (mm), which was measured at five sites for each push-out sample with a digital caliper micrometer. The values reported are the mean of the five measurements.

After the push-out tests the retrieved implants were pulled-out completely from the surrounding bone tissue and were placed in clean and sterile plastic containers filled with saline solution. The retrieved implants and the wet tissue that was in direct contact with the implant were dehydrated with 100% acetone for 15 minutes, baked at 180°C, mounted on aluminum stub using carbon tape and coated with a thin layer of carbon to be examined by SEM/EDX.

Statistical Analyses

Values of interfacial shear strength are given as the mean ± standard deviation (SD) and were assessed using one-way analysis of variance at a significance level of 5%, then compared among specimens by Tukey's test at a significance level of 5%.

RESULTS

Surface Characterization and Zn Ion Release Test

Figure 2 presents the typical surface morphology of unmodified-Ti (see Figure 2A) and after the different surface modifications (see Figure 2B–D) Grinding grooves were observed on the mechanically abraded surfaces (see Figure 2, B and D). A reticulated microporous structure was obtained after immersion in the alkali solution containing the $[Zn(OH)_4]^{2-}$ complex at 60°C for 24 hours (see Figure 2C). The combination of MGT and the surface treatment with an aqueous solution containing the $[Zn(OH)_4]^{2-}$ complex produced a duplex surface consisting of grinding grooves with a reticulated microporous structure (see Figure 2D). In groups III and IV, EDX measurements indicated the presence of Zn in the surface of approximately 2 at.%. The average surface roughness (R_a) and peak-to-valley height (R_z) increased by means of the immersion in the alkali solution. The average surface roughness of the control group (group I) exhibited the lowest roughness, whereas the samples of group II showed the highest values (Figure 3). In groups III and IV the alkali solution containing the $[Zn(OH)_4]^{2-}$ complex produced a porous surface with roughness measured on a micrometer scale

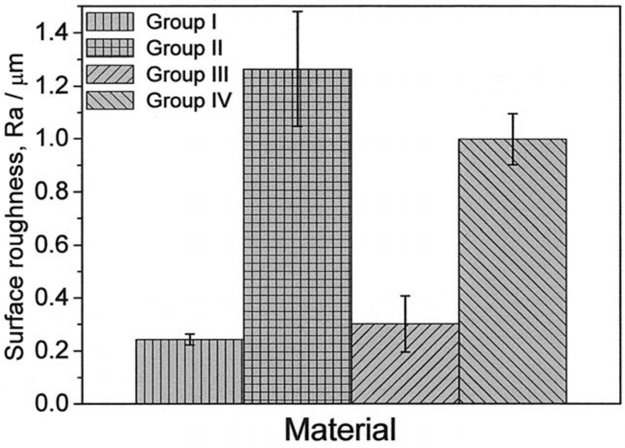

Figure 3 Average surface roughness (R_a) of the different evaluated materials. Error bars represent the standard deviation; $n = 3$. 145 × 104 mm (300 × 300 DPI).

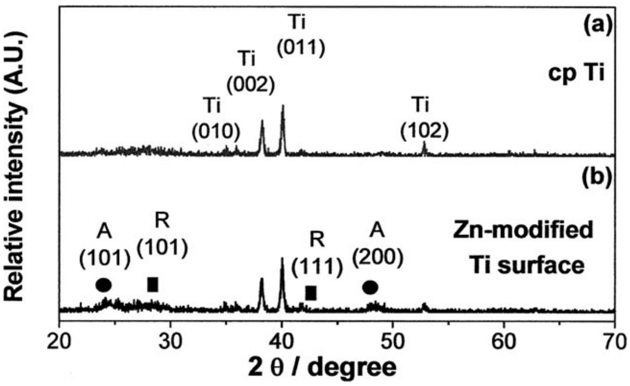

Figure 5 TF-XRD patterns for the titanium specimens: cp-Ti autoclaved at 121°C for 30 minutes (A), cp-Ti after immersion in the alkali solution containing $[Zn(OH)_4]^{2-}$ ions (B). The diffraction peaks for the anatase and rutile phases are labeled “A” and “R,” respectively, with the corresponding diffraction planes given in parentheses. 138 × 87 mm (300 × 300 DPI).

and the MGT produced a surface that was significantly rougher compared with the alkali-treated sample ($p < 0.001$) (see Figure 3).

No measurable Zn content was detected by ICP in the samples treated with the alkali solution containing the $[Zn(OH)_4]^{2-}$ complex within the first 6 hours of soaking in physiological saline (Figure 4). This fact suggests that the concentration of Zn released was under the detection limit at the beginning of the experiment. However, at prolonged soaking times, the Zn concentration in the physiological saline increased reaching 13.2 µg/l (0.20 µM) after 168 hours (see Figure 4).

In the TF-XRD patterns of the steam sterilized titanium and the titanium specimen immersed in the alkali solution containing the $[Zn(OH)_4]^{2-}$ complex solution the predominant reflections in both profiles were the α-Ti reflections at 35.1°, 38.4°, 40.2°, 53.0°, and 70.7° in 2θ (JCPDS card: 44-1294) (Figure 5). Four very weak peaks that could be assigned to anatase-TiO_2 (101), anatase-TiO_2 (200), rutile-TiO_2 (101), and rutile-TiO_2 (111) were also present in the profile of the alkali-modified sample. In contrast, in the steam sterilized sample is possible that amorphous oxide or oxyhydroxides of titanium were present in the titanium surface. Interestingly, we did not observe the formation of a sodium titanate phase on the surface of the samples treated with the alkali solution containing $[Zn(OH)_4]^{2-}$ complex. Moreover, in the surface layer Na was not detected by neither EDX nor XPS analyses.

The XPS survey spectrum of the control revealed the presence of Ti, O, and C as surface contamination, suggesting that the surface oxide of the control is mainly TiO_2. On the other hand, Ti, Zn, and O were detected in the specimens after the alkali modification (Figure 6). Small amounts of C, Ca, and Mg were registered and are considered impurities. It should be noted that Na was not found in the surface of the alkali-modified titanium sample. Higher resolution narrow-scan spectra were measured for the Ti, Zn, and O1s at a 50 eV pass energy. Figure 7, A–C show the variation of the characteristic peaks of Ti 2p, Zn 2p, and O 1s with depth. Figure 7A shows the spectra of Ti 2p energy region, which consists dominantly of a doublet peak at 459 eV (for titanium oxide $Ti2p_{3/2}$) and 464.8 eV (for titanium oxide $Ti2p_{1/2}$), respectively. These two major peaks can be attributed to

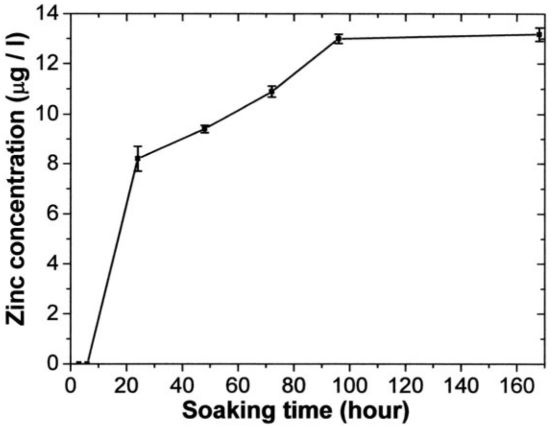

Figure 4 Zinc release in physiological solution. Specimens immersed in the alkali solution containing the $[Zn(OH)_4]^{2-}$ complex solution were soaked in 100 mL of physiological saline solution (0.9% NaCl, pH 7.4) and checked for Zn^{2+} release at different soaking times. 139 × 109 mm (300 × 300 DPI).

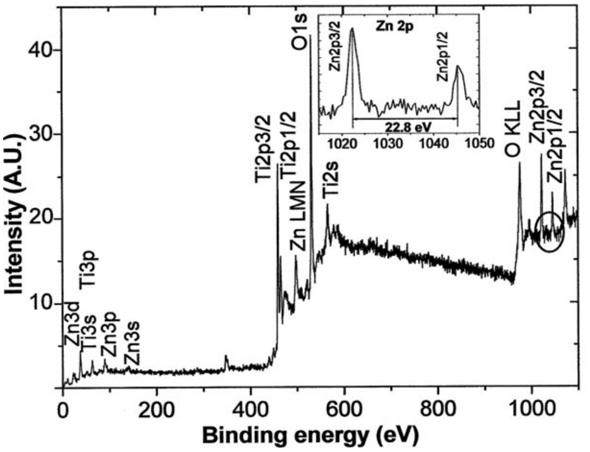

Figure 6 Survey XPS spectra of cp-Ti after immersion in the alkali solution containing $[Zn(OH)_4]^{2-}$ ions. The inset shows the Zn2p region for cp-Ti after immersion in the alkali solution containing $[Zn(OH)_4]^{2-}$ ions. 147 × 118 mm (300 × 300 DPI).

the tetravalent titanium form such as TiO_2. Intensity of the peaks because of Ti^{4+} from TiO_2 decreased with an increase in the Ar^+ ion etching time. At 400 nm a doublet corresponding to a low oxidation state of Ti was observed. A broad shoulder around 455 eV for the titanium metal $Ti2p_{3/2}$ and around 460 eV for the titanium metal $Ti2p_{1/2}$ peak was observed. The peak corresponding to O 1s is shown in Figure 7B and appeared at 531.00 eV. The XPS O 1s peak shows an asymmetrical broadening in the range of 530.4 to 535.7 eV, implying that at least two types of oxygen species are present in the near surface region.[18] On the other hand, the development of the O 1s peaks with depth shows a decreasing intensity with increasing depth. Asymmetrical broadening of the O 1s peak may be deconvoluted into a peak at 532.4 eV related to the OH (for example, from chemisorbed H_2O or surface hydroxyl species)[19–21] and a peak near 531 eV, attributed to nonstoichiometric Zn-O bond.[22] Usually a binding energy in the O 1s peak at 530.2 eV is attributed to the O^{2-} ions in the wurtzite structure of hexagonal Zn^{2+}.[23] In our case, the offset in the binding energy to a higher value indicates that the oxygen bonding is stronger than the stoichiometric Zn-O bond and hence, at the interface the Zn-O interatomic distance is shorter than in the stoichiometric

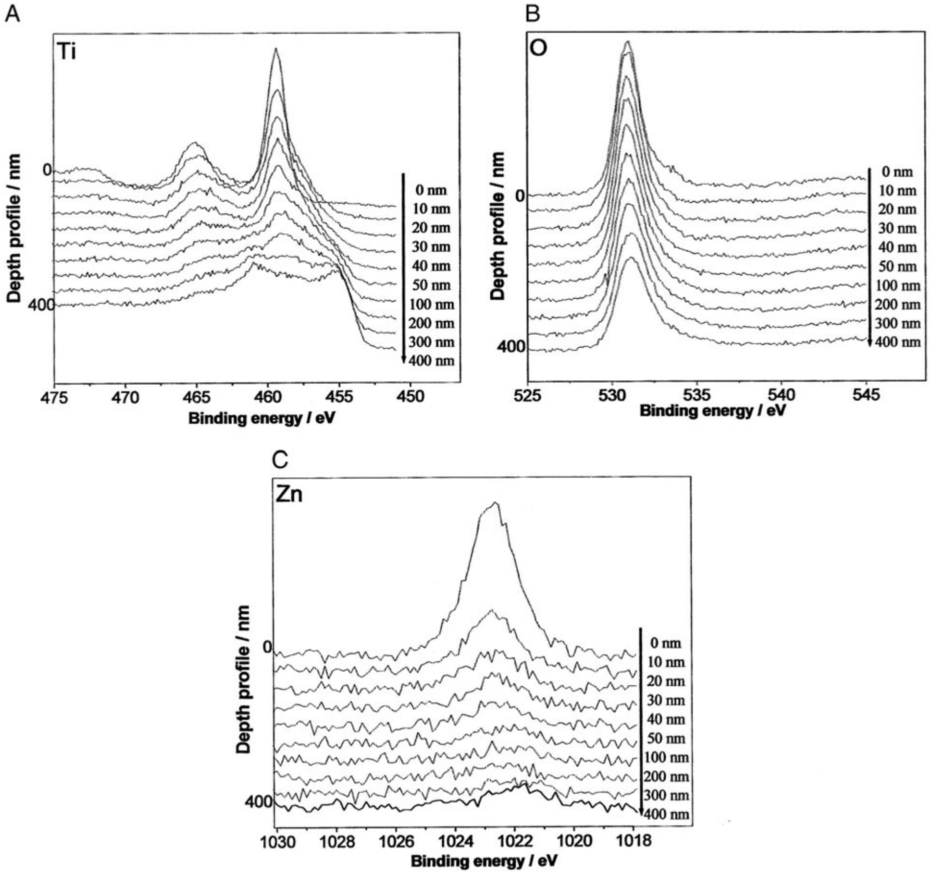

Figure 7 Elemental composition of Ti, O, and Zn of the cp-Ti after immersion in the alkali solution containing $[Zn(OH)_4]^{2-}$ ions as a function of depth; Ti 2p region (A), O 1s region (B), Zn 2p region (C). 204 × 190 mm (300 × 300 DPI).

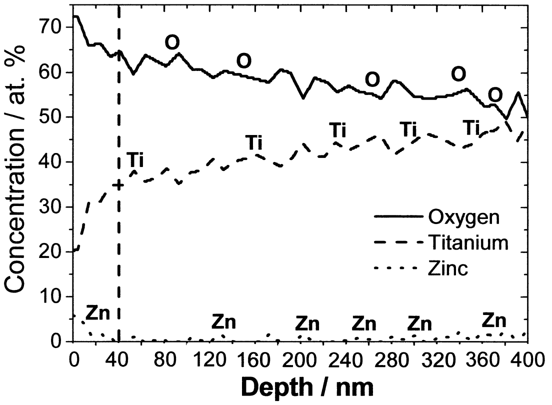

Figure 8 ESCA depth profiles of cp-Ti after immersion in the alkali solution containing $[Zn(OH)_4]^{2-}$ ions. 168 × 131 mm (300 × 300 DPI).

Zn-O bonds. This interpretation can be found also in the XPS O 1s binding energy database compiled by The National Institute of Standards and Technology.[24]

The XPS peak for Zn $2p_{3/2}$ is sharp (see Figure 7C), does not show an asymmetric feature and appeared at 1022.4 eV, indicating only divalent Zn^{2+} exists on the surface.[16] The Zn 2p peak contributions to the XPS spectrum, Zn $2p_{1/2}$ (1045.2 eV) and Zn $2p_{3/2}$ (1022.4 eV) are shown in the inset of Figure 6. It was interesting to find that the difference between the two peaks gave a spin orbit coupling of 22.8 eV, lower than the reported in the literature for ZnO (≈ 23.1 eV).[24,25]

The change of the surface chemistry after immersion in the alkali solution containing the $[Zn(OH)_4]^{2-}$ complex was evaluated by ESCA (electron spectroscopy for chemical analysis; Perkin-Elmer Co., USA) depth profiles (Figure 8). The composition (in at.%) of the Zn-modified surface is approximately 20.02 %Ti, 73.98. %O, and 6.0 % Zn. The oxygen profile suggests that the amount of surface oxidation decreases with the increasing in depth. According to the depth profile, the thickness of the oxide layer is more than 400 nm, because nearly 50 at.% of oxygen is still present at 400 nm. In the outermost surface layer Zn is present in about 6 at.% and disappeared at about 40 nm. The carbon content is regarded as a surface contaminant since it disappeared to noise levels after Ar^+ ion sputter cleaning, corresponding to approximately 20 nm (carbon signal not shown). Figure 9 schematically indicates the ionic bonding at the interface suggested for the cp-Ti treated with the alkali solution containing the $[Zn(OH)_4]^{2-}$ complex. The analysis of the XPS data suggests the formation of a Ti-O-Zn-O-H bond.

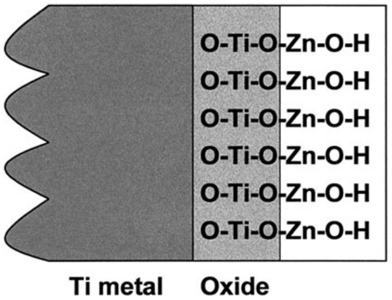

Figure 9 Schematic diagram in cross-section of the ionic binding at the interface of the titanium metal treated with the alkali solution containing $[Zn(OH)_4]^{2-}$ ions. 136 × 109 mm (300 × 300 DPI).

Clinical Observations

All animals tolerated the surgery well and survived until the final experimental time. Macroscopically, no signs of inflammation, infection or adverse tissue reaction were observed around any of the implants. A periosteal/ endosteal callus covered the external lateral and intramedullary surfaces of all the cylindrical implants. Even after 4 weeks of implantation the alkali-modified implants were rigidly anchored in their bony seats.

Biomechanical Testing and SEM Observation

The results of the biomechanical tests for all implants types, mean push-out shear strength values at the different time periods, and statistical significance ($p < 0.05$) are shown in Figure 10. The alkali treatment containing

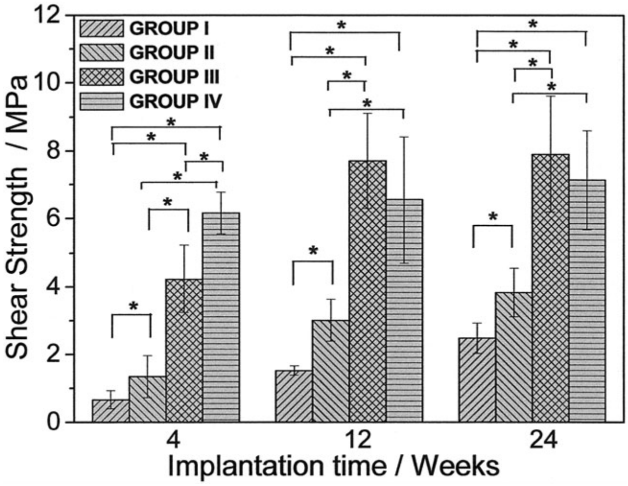

Figure 10 Interface shear strength between bone and the different evaluated Ti implants with the implantation time. Values are the mean ± SD ($n = 5$). (* indicate a statistically significant difference among implant materials, $p < 0.05$.) 152 × 119 mm (300 × 300 DPI).

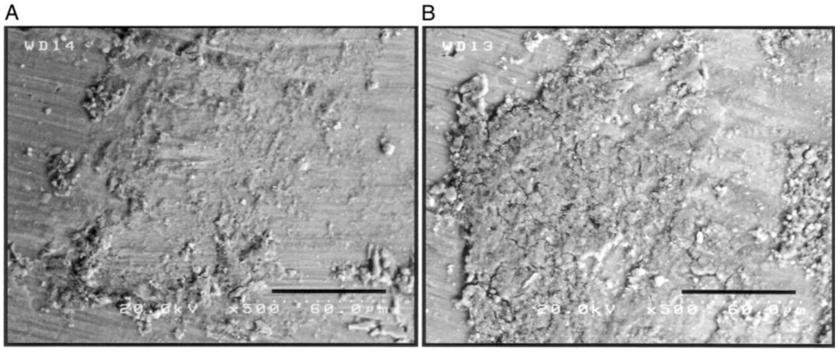

Figure 11 Scanning electron micrographs showing bone remnants in the surface of the implants treated with the alkali solution containing $[Zn(OH)_4]^{2-}$ ions after the push-out test for the implantation of 24 weeks: smooth surface (group III) (A), mechanically grinded surface (group IV) (B). The implants were partly covered by bone that is firmly attached to the surface, which indicates strong bonding between the implant and bone. 153 × 59 mm (300 × 300 DPI).

$[Zn(OH)_4]^{2-}$ complex applied in this study significantly increased the implant-bone shear strength after all the implantation periods. The multiple comparisons of the push-out shear strength values using one-way analysis of variance and the Tukey test demonstrated that there were statistically significant differences among groups I–II, groups I–III, and groups I–IV at all the healing times.

After 4 weeks, the push-out test values of the control implants were less than 1 MPa (0.66 ± 0.27 MPa). The same titanium smoothed surface but modified by the immersion into the alkali solution containing the $[Zn(OH)_4]^{2-}$ complex exhibited a significantly higher mean value (4.23 ± 0.99 MPa, $p = 0.009$). Extra bone anchorage was obtained at 4 weeks by means of the applied MGT treatment to the implants modified with the $[Zn(OH)_4]^{2-}$ complex (6.16 ± 0.62 MPa, $p = 0.002$). However, after 12, 24 weeks there were no statistically significant differences in push-out shear strength values between groups III and IV ($p = .79$ and $p = .22$, respectively).

After 24 weeks, the increase in the shear strength was less than at 12 weeks and the maximum shear strength value was reached by the implants of group III (9.308 MPa, $p = 0.001$).

Figure 11 shows the FESEM morphologies of the surface of the implants modified with the $[Zn(OH)_4]^{2-}$ complex after the push-out test. It was observed that bone remnants adhered to the surface of the alkali-modified implants. In the $[Zn(OH)_4]^{2-}$ complex-modified mechanically grinded surface the bone remnants were more abundant, while in the nontreated Ti implants (group I and group II) bone remains were not observed. Therefore, the shear strength between the $[Zn(OH)_4]^{2-}$ complex-modified implants and bone is higher than the bone itself.

DISCUSSION

The applied Ti alkali treatment with an alkali solution containing the $[Zn(OH)_4]^{2-}$ complex modified the morphology and roughness (topography) of the surface, increased the surface oxide thickness and changed the chemical composition and the crystalline structure of the titanium oxide (TiO_2). This modification resulted in a strongest bone-implant fixation response regarding push-out test between the four groups after 24 weeks of implantation time. An important factor that helps to retain the implant inside the bone is the surface topography because the rougher the implant, the higher the physico-chemical and biological contact available to produce adhesion at the interface. We suppose that after 4 weeks of implantation time the increase in push-out values with the increasing of surface roughness is because of a mechanical interlocking with the newly formed bone. Nevertheless, the manner in which titanium interacts with bone is complex and not only dependent on surface topography. Other factors such as the chemical composition of the surface play a crucial role in early stages of bone formation. The present study demonstrated that Zn-modified titanium surface greatly influenced the bone tissue response. Zn concentration above 5.88 mg/L may have serious cytotoxic effects on cells.[26] In this study, Zn^{2+} ion release could be detected in vitro and its concentration was below the concentration that has been shown to inhibit normal osteoblasts function. Furthermore, it has been reported in several studies that Zn in the micromolar concentration range is found to have positive roles in promoting bone formation and inhibiting bone resorption.[6] Furthermore, even though after the alkali treatment without heat treatment was applied, the cp-Ti treated with the alkali solution containing the $[Zn(OH)_4]^{2-}$ complex produced an oxide film of more than 400 nm, which was stable against the Ar^+ ion bombardment. Alteration in the surface oxide thickness may have lead to increased bone apposition and stronger bone fixation as well.

In addition, from the TF-XRD measurements it can be seen that unlike the conventional alkali and heat treatment modification, in our Ti samples treated with the alkali solution containing the $[Zn(OH)_4]^{2-}$ complex a sodium titanate layer was not formed. Instead of this, crystalline TiO_2 layers of anatase-TiO_2 and rutile-TiO_2 were formed. Several studies have revealed that a titania layer with specific crystalline structures (e.g., anatase) on the sodium-free bioactive titanium is more bioactive that sodium titanate layer.[27,28] Indeed, enhanced in vitro bioactivity and in vivo bone formation have been observed in sodium-free alkali and heat-treated Ti with an external layer of anatase and rutile.[28] For our implants, it is likely that the improved bone-implant fixation obtained after the applied surface modification is explained not only by the external surface layer crystallinity change but also by the increase of the surface oxide thickness and the modified chemical composition of the outermost layer together with the topography surface changes that were introduced after the surface modification.

The effect of different surface treatments applied to Ti in the push-out shear strength can be seen in Table 1. The results obtained from different studies are difficult to compare, though, we have compiled data corresponding to cylindrical-type implants inserted using a transcortical model, which also used the push-out test to evaluate implant fixation. Our shear strength data revealed that the achieved values in the implants treated with the alkali solution containing the $[Zn(OH)_4]^{2-}$ complex are appreciably higher than the values obtained after a traditional alkali heating and heat treatment modification even though the surface roughness (R_a) of our implants was lower. Mechanical evaluation of extracted hydroxyapatite (HA-) coated implants has shown evidence of increased interfacial strength compared with implants with bare Ti surfaces.[30–32] However, the shear strength values achieved in this study were

TABLE 1 Comparison Among the Bone-Implant Shear Strength Achieved in the Present Study and in Similar Investigations

Authors	Biomaterial/Animal Model	Surface Treatment	Surface Roughness (R_a) (μm)	Healing Time (weeks)	Interface-Shear Strength (MPa)
Nishiguchi et al.[17]	Titanium rods/dog femurs	Alkali-heating (AH) with NaOH and heat treatment vs nontreated	1.09 vs 1.16	12	3.24 ± 2.11 vs 1.24 ± 1.05
Svehla et al.[29]	Ti6Al4V dowels/sheep tibiae	Smooth vs grit-blasted	0.28 vs 5.68	12	1 ± 1 vs 10 ± 3
Ozeki et al.*[30]	Titanium rods/dog femurs	Hydroxyapatite sputter-coated vs noncoated titanium	–	12	3.5 vs 1.0
Maxian et al.*[31]	Titanium rods/rabbit femurs	Crystalline hydroxyapatite plasma spray-coated vs noncoated smooth titanium	–	12	6.244 vs 0.858
Hayashi et al.[32]	Titanium rods/dog femurs	Rough hydroxyapatite coated titanium	3.4 vs 8.4	12	5.70 vs 13.3
Li et al.[33]	Titanium rods/rabbit tibiae	Machined vs dimpled surface (140 μm diameter dimple)	1.5	12	4.0 vs 10.8
This work	Titanium rods/rabbit femurs	Ti smooth vs Ti grinded vs Ti after AH with $[Zn(OH)_4]^{2-}$ complex (smooth) vs Ti after AH with $[Zn(OH)_4]^{2-}$ complex (grinded surface)	0.24 vs 1.26 vs 0.30 vs 0.99	12	1.52 vs 3.01 vs 7.70 vs 6.56

Note: The studies showed here were carried out using a cylindrical-type implant (transcortical model) and the test used to evaluate the implant fixation was the push-out test.
*R_a value not provided.

superior to studies in which the titanium surface was coated with HA by radio frequency magnetron sputtering or plasma-spraying.[30,31] The obtained results indicate that the changes in the surface chemistry composition promoted a biochemical bonding at the bone-implant interface stronger than the one obtained after HA coating, improving the implant fixation. The strong bonding could be evidenced also by the presence of bone remains after the push-out test. The alkali-modified implants were partly covered by bone that was firmly attached to the surface, which indicates strong bonding between the implant and bone.

It is difficult to state presently the mechanism that lead to strong bone bonding in our chemically and topographically modified implants. However, the results of this research could stimulate further research aimed to explain the relationship between the Zn surface modification and the increased bone fixation.

CONCLUSION

The surfaces treatment applied using an alkali solution containing the $[Zn(OH)_4]^{2-}$ complex presented an improvement in bone-implant attachment over the control group (cp-Ti smooth surface or mechanically grinded surface), increasing the osseointegration of the titanium surface during the early stages of bone regeneration. The obtained results support the idea that a Ti surface with a particular topography and crystalline oxide layer with an increased thickness, together with the implementation of a chemical surface treatment that allows Zn^{2+} ion release can be useful for improving the biological fixation of bone implants. The applied surface treatment can be easily carried out and does not require a secondary step of high temperature heat treatment. The possibilities of increasing Zn release rate by controlling the surface roughness will be explored in further research. More extensive in vitro as well as in vivo studies to assess the biological responses to these chemically and topographically modified Ti surfaces are ongoing.

CONFLICT OF INTEREST STATEMENT

The authors have no conflicts of interest to declare. [Correction added after online publication 24 May 2010: Conflict of Interest Statement added.]

REFERENCES

1. Yan WQ, Nakamura T, Kobayashi M, Kim HM, Miyaji F, Kokubo T. Bonding of chemically treated titanium implants to bone. J Biomed Mater Res 1997; 37:267–275.
2. Fujibayashi S, Nakamura T, Nishiguchi S, et al. Bioactive titanium: effect of sodium removal on the bone-bonding ability of bioactive titanium prepared by alkali and heat treatment. J Biomed Mater Res 2001; 56:562–570.
3. Gou Z, Weng W, Yan W, Du P, Han G, Wang Z. A novel route to fabricate the biomedical material: structure strategy and the biologically active ions controllable release. J Control Release 2006; 116:360–364.
4. Okazaki M. New type of scaffold biomaterials with magnesium accelerating osteoblast adhesion and bone formation. J Oral Tissue Eng 2004; 1:31–40.
5. Anderson PA, Copenhaver JC, Tencer AF, Clark JM. Response of cortical bone to local controlled release of sodium fluoride: the effect of implant insertion site. J Orthop Res 1991; 9:890–901.
6. Yamaguchi M. Role of zinc in bone formation and bone resorption. J Trace Elem Exp Med 1998; 11:119–135.
7. Yamaguchi M, Inamoto K, Suketa Y. Effect of essential trace metals on bone metabolism in weanling rats: comparison with zinc and other metals action. Res Exp Med 1986; 186:337–342.
8. Yamaguchi M, Oishi H, Suketa Y. Stimulatory effects of zinc on bone formation in tissue culture. Biochem Pharmacol 1987; 36:4007–4012.
9. Yamaguchi M. β-alany-L-histidinate zinc and bone resorption. Gen Pharmacol 1995; 26:1179–1183.
10. Yamaguchi M. β-alany-L-histidinate zinc: a potent activator in bone formation. Curr Med Chem 1995; 1:356–365.
11. Moonga BS, Dempster DW. Zinc is a potent inhibitor of osteoclastic bone resorption in vitro. J Bone Miner Res 1995; 10:453–457.
12. Hashizume M, Yamaguchi M. Stimulatory effect of β-alany-L-histidinate zinc on cell proliferation is dependent on protein synthesis in osteoblastic MC3T3-E1 cells. Mol Cell Biochem 1993; 122:59–64.
13. Yamaguchi M, Kishi S, Hashizume M. Effect of zinc-chelating dipeptides on osteoblastic MC3T3-E1 cells: activation of aminoacyl-tRNA synthetase. Peptides 1994; 15:1367–1371.
14. Albrektsson T, Wennerberg A. Oral implant surfaces: part I – review focusing on topographic and chemical properties of different surfaces and in vivo responses to them. Int J Prosthodont 2004; 17:536–543.
15. Larsson C, Thomsen P, Lausmaa J, Rodahl M, Kasemo B, Ericson LE. Bone response to surface modified titanium implants: studies on electropolished implants with different oxide thicknesses an morphology. Biomaterials 1994; 15:1062–1074.
16. Bobyn JD, Stackpool JG, Hacking SA, Tanzer M, Krygier JJ. Characteristics of bone ingrowth and interface mechanics of

a new porous tantalum biomaterial. J Bone Joint Surg Br 1999; 81-B:907–914.

17. Nishiguchi S, Kato H, Fujita H, et al. Titanium metals form direct bonding to bone after alkali and heat treatments. Biomaterials 2001; 22:2525–2533.
18. Hou X, Zhou F, Yu B, Liu W. Superhydrophobic zinc oxide surface by differential etching and hydrophobic modification. Mater Sci Eng A 2007; 452–453:732–736.
19. Gopel W, Anderson JA, Frankel D, et al. Surface defects of TiO2 (110): a combined XPS, XAES and ELS study. Surf Sci 1984; 139:333–346.
20. Shirkhanzadeh M. XRD and XPS characterization of superplastic TiO_2 coatings prepared on Ti6Al4V surgical alloy by an electrochemical method. J Mater Sci Mater Med 1995; 6:206–210.
21. Shibata T, Zhu YC. The effect of film formation conditions on the structure and composition of anodic oxide films on titanium. Corros Sci 1995; 37:253–270.
22. Pugel DE, Vispute RD, Hullavarad SS, Venkatesan T, Varughese B. Compositional origin of surface roughness variations in air-annealed ZnO single crystals. Appl Surf Sci 2008; 254:2220–2223.
23. Saw KG, Ibrahim K, Lim YT, Chai MK. Self-compensation in ZnO thin films: an insight from X-ray photoelectron spectroscopy, Raman spectroscopy and time-of-flight secondary ion mass spectroscopy analyses. Thin Solid Films 2007; 515:2879–2884.
24. National Institute of Standards and Technology (NIST). NIST X-ray Photoelectron Spectroscopy Database. 2007. http://srdata.nist.gov/xps/Default.aspx.
25. Maiti UN, Ahmed SkF, Mitra MK, Chattopadhyay KK. Novel low temperatures synthesis of ZnO nanostructures and its efficient field emission property. Mater Res Bull 2009; 44:134–139.
26. Yamamoto A, Honma R, Sumita M. Cytotoxicity evaluation of 43 metal salts using murine fibroblasts and osteoblastic cells. J Biomed Mater Res 1998; 39:331–340.
27. Uchida M, Kim HM, Kokubo T, Fujibashi S, Nakamura T. Effect of water treatment on the apatite forming ability of NaOH-treated titanium metal. J Biomed Mater Res 2002; 63:522–530.
28. Takemoto M, Fujibayashi S, Neo M, et al. Osteoinductive porous titanium implants: effect of sodium removal by dilute HCl treatment. Biomaterials 2006; 27:2682–2691.
29. Svehla M, Morberg P, Zicat B, Bruce W, Sonnabend D, Walsh WR. Morphometric and mechanical evaluation of titanium implant integration: comparison of five surface structures. J Biomed Mater Res 2000; 51:15–22.
30. Ozeki K, Yuhta T, Aoki H, Nishimura I, Fukui Y. Push-out strength of hydroxyapatite coated implants by sputtering technique in bone. Biomed Mater Eng 2001; 11:63–68.
31. Maxian SH, Zawadsky JP, Dunn MG. Mechanical and histological evaluation of amorphous calcium phosphate and poorly crystallized hydroxyapatite coatings on titanium implants. J Biomed Mater Res 1993; 27:717–728.
32. Hayashi K, Inadome T, Tsumura H, Nakashima Y, Sugioka Y. Effect of surface roughness of hydroxyapatite-coated titanium on the bone-implant interface shear strength. Biomaterials 1994; 15:1187–1191.
33. Li J, Liao H, Fartash B, Hermansson L, Johnsson T. Surface-dimpled commercially pure titanium implant and bone ingrowth. Biomaterials 1997; 18:691–696.